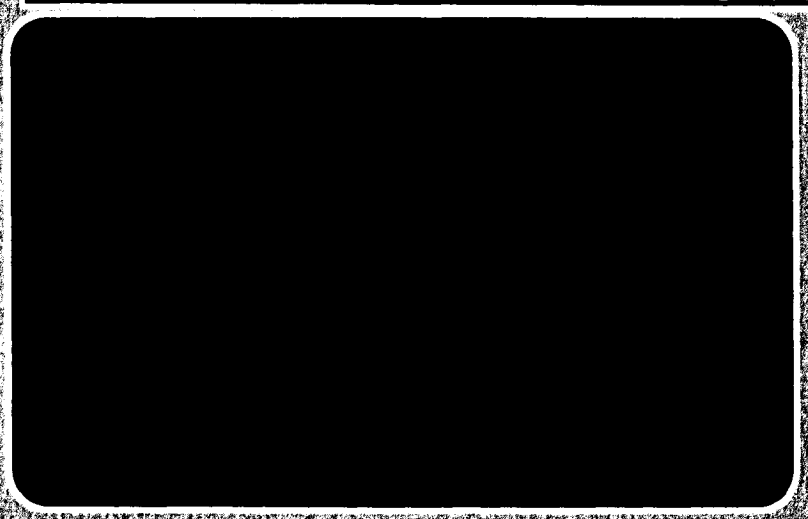

TU Delft
Delft University of Technology
Faculty of Aerospace Engineering

Memorandum M-725

CONCEPTUAL DESIGN OF A 70 PASSENGER AIRLINER PROPELLED BY FUEL-EFFICIENT TURBOFAN ENGINES

S.H.J.A. Fransen

GARTEUR AG meeting, Bremen, Germany
March 19-20, 1996

CONCEPTUAL DESIGN OF A 70 PASSENGER AIRLINER PROPELLED BY FUEL-EFFICIENT TURBOFAN ENGINES

by

S.H.J.A. Fransen
Faculty of Aerospace Engineering
Delft University of Technology
P.O. Box 5058, 2600 GB Delft
The Netherlands

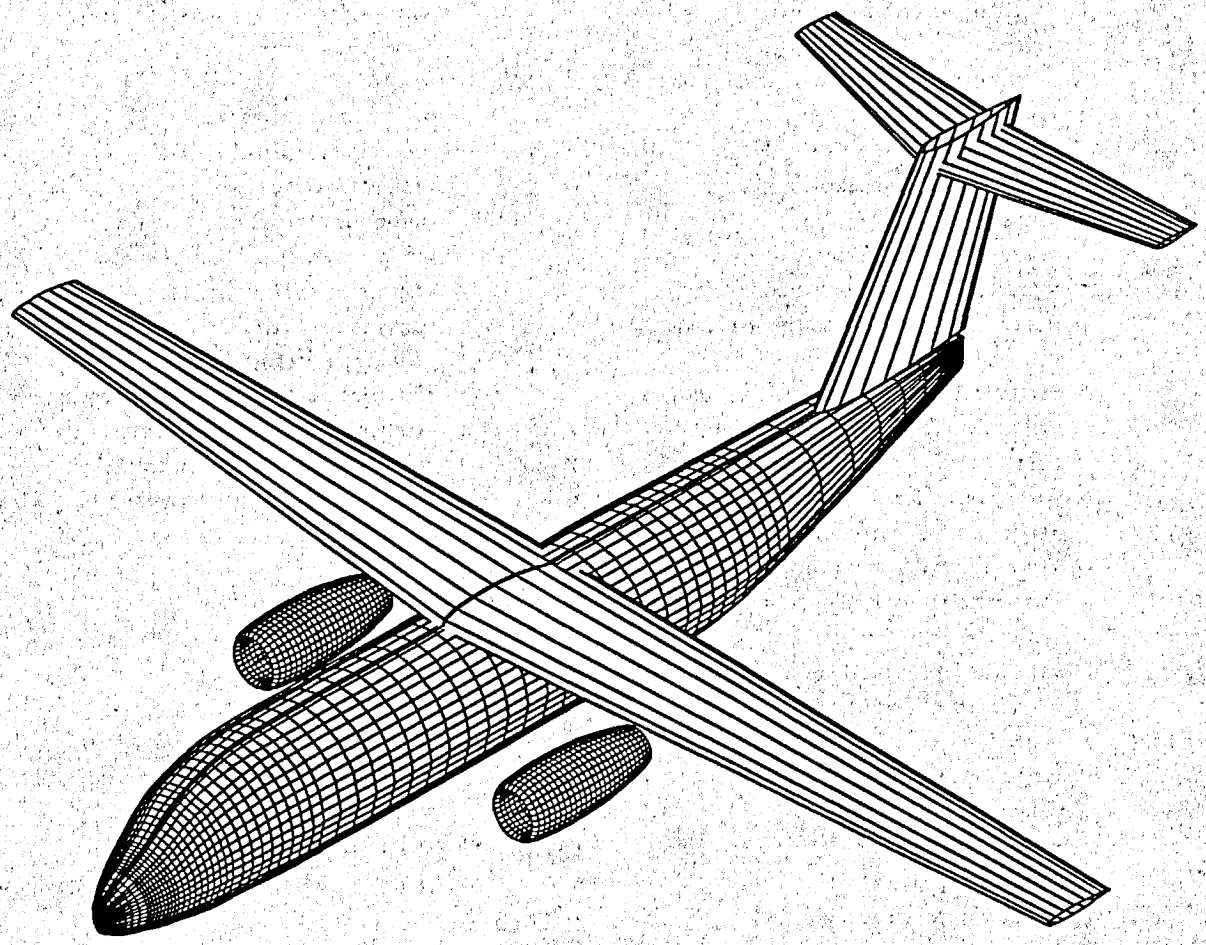

Aircraft design study in accordance with the GARTEUR exploratory project on "Multi-Disciplinary Wing Optimization".
Participants:
Aerospatiale - France, AVRO - UK, BAe (civil) - UK, BAe (military) - UK, DASA (München) - Germany, Deutsche Airbus - Germany, DRA - UK, NLR - The Netherlands, SAAB - Sweden, SAMTECH - France, TUD - The Netherlands

Nomenclature

symbols

a	=fuel price per unit weight
$\bar{a}$	=deceleration
A	=aspect ratio
A_h	=aspect ratio of horizontal tail plane
A_v	=aspect ratio of vertical tail plane
b	=wing span
b_{ail}	=aileron span
BFL	=Balanced Field Length
c	=local chord
$\bar{c}$	=mean aerodynamic chord
c_{c_f}	=flight crew hourly costs
c_{m_t}	=flight trip maintenance costs
C	=climb ratio
C_0	=equivalent C_{D_0} for take-off configuration
C_p	=pressure coefficient
C_D	=drag coefficient
C_{D_0}	=zero-lift drag coefficient
C_L	=lift coefficient
$C_{L_{max}}$	=maximum lift coefficient
C_T	=thrust specific fuel consumption
D	=aircraft drag, depreciation period [years]
DOC	=Direct Operating Cost
e	=Oswald factor for clean configuration
E	=equivalent Oswald factor for take-off configuration
f_{land}	=safety factor for landing distance
f_{TO}	=safety factor for take-off distance
g	=acceleration due to gravity
h_{land}	=screen height for landing
h_{TO}	=screen height for take-off
l_h	=arm length of vertical tail AC to wing AC
l_v	=arm length of vertical tail AC to wing AC
L	=aircraft lift
$\dot{m}$	=engine intake mass flow
M	=Mach number
M_c	=cruise Mach number
N_e	=number of engines
N_{pax}	=number of passengers
p	=static air pressure
R	=range, gas constant
S	=gross wing surface area
S_{ail}	=aileron area
S_h	=gross area of horizontal tail plane
S_{land}	=landing distance
S_v	=gross area of vertical tail plane
S_{TO}	=take-off distance to screen height
t	=local maximum airfoil thickness
t_b	=block time [hours]
T	=thrust
T_0	=static temperature sea level ISA
$\bar{T}$	=mean thrust during take-off run
T_{TO}	=take-off thrust
U	=annual utilisation [hours]
V_2	=take-off safety speed one engine inoperative
V_{ail}	=aileron volume coefficient
V_h	=horizontal tailplane volume coefficient
V_v	=vertical tailplane volume coefficient
V_s	=stalling speed
W_e	=weight of engine core
W_{land}	=maximum landing weight
W_w	=wing structural weight
W_F	=fuel weight
W_{OE}	=operational empty weight
W_P	=pay-load
W_{TO}	=maximum take-off weight
W_{ZF}	=maximum zero fuel weight
γ	=ratio of specific heats
γ_{LOF}	=lift-off angle of climb
λ	=by-pass ratio, taper ratio of wing
λ_h	=taper ratio of horizontal tail
λ_v	=taper ratio of vertical tail
$\Lambda_{1/4}$	=wing quarter chord sweep angle
$\Lambda_{h_{1/4}}$	=horizontal tail quarter chord sweep angle
$\Lambda_{v_{1/4}}$	=vertical tail quarter chord sweep angle
μ	=equivalent ground friction coefficient
θ	=relative atmospheric temperature
ρ	=air density

Abbreviations

AC	=Aerodynamic Centre
CG	=Centre of Gravity
CAD	=Computer Aided Design
ADAS	=Aircraft Design and Analysis System
ISA	=International Standard Atmosphere
FAR	=Federal Aviation Regulations
JAR	=Joint Airworthiness Regulations

Abstract

The conceptual design process of a regional transport airliner, intended to carry a design pay-load of 70 passengers plus baggage over a distance of 2500 km, will be described. The design cruise Mach number will be M=0.70 at an altitude of 30000 ft. In fact 6 different aircraft will be designed to allow a discrete variation of the primary design variable, which is the wing aspect ratio. The aspect ratio varies from 8 to 15.5 by an increment of 1.5.

To limit the amount of changes in the overall aircraft design it was decided that the fuselage and tail design

should be the same under variation of the aspect ratio. Also longitudinal and spanwise engine position will be fixed. On the contrary the wing design will be different for the 6 designs and wing position might vary as well.

The aircraft is to be optimized for maximum range and direct operating cost. In the design procedure the maximum take-off weight will be kept constant. Finally the wing area should be constant as well, which implies a certain constant wing loading has to be chosen for the family of 6 designs. By keeping W_{TO} constant, the range will vary as a function of the aspect ratio, because wing structural weight, fuel weight, engine weight and L/D are all dependent on aspect ratio. Different optimum aspect ratios for maximum range and DOC are derived.

Introduction

The design procedure will be split up into several parts in the following chapters. The fuselage design procedure will be described first, for which a CAD design program was used. Furthermore planform design and performance requirements will be discussed. For the purpose of designing the planform a program has been developed which allows the user to design the planform for a specified number of input variables listed in a standard input file. The program has been implemented into the ADAS system. The program also generates a drawing of the planform geometry written in DXF (Data Exchange Format), drag polars, glide ratio curves, thrust to weight ratio versus wing loading diagrams, lift distribution plots, load and balance diagrams and sensitivity graphs. All plots are generated for six different aspect ratios, except for the sensitivity plots which give gradient information for certain dependent variables as function of the aspect ratio. The architecture of the design program and its application will be discussed. A sensitivity analysis for wing weight, fuel weight, engine weight, range and DOC as a function of aspect ratio will be performed for constant W_{TO}.

Aircraft Specification

In this chapter the aircraft specification will be given. It has been split up into several subjects.

Range and Capacity

The design pay-load will be 70 passengers including their luggage plus freight. A passenger weighs 80 kg and a passenger's baggage has a weight of 20 kg. The freight weight is specified as 1400 kg and has a density of 150 kg/m^3. The total pay-load will therefore total 8400 kg. The design range will be 2500 km with maximum pay-load.

Propulsion

The aircraft should be a twin-engine design. For this purpose two high by-pass ratio turbofans or propfans should be used to minimize environmental noise, fuel consumption and emissions. To allow the choice of different engines a high-wing configuration will be beneficial. Initially the performance data of the Rolls Royce - SNECMA RB410 have been used which, in a later stage, might be replaced by another turbofan or propfan design. For reasons of the outdated RB410 specification (1972), a weight of 1.1 times the weight of a Rolls Royce Tay Mk620 engine with a take-off thrust of T_{TO}=61.3 kN might be used. Engine weight and take-off thrust might be scaled for the various designs. Finally the BMW-Rolls Royce BR512 project engine will be used with a take-off thrust of T_{TO}=60.1 kN and a by-pass ratio of 5.

Cockpit

The cockpit is designed for a two-man crew. All instruments and controls necessary for the safe conduct of flights are within easy sight and reach of each of the pilots. Downward vision over the nose should be at least 17 degrees. Also the wing tip must be visible for varying aspect ratio, without change of the cockpit windscreen design.

Fuselage Lay-out

Cabin

The pressure cabin altitude will be 8000 ft (2440 m) and the maximum cruise altitude (service ceiling) will be constrained to 35000 ft (10670 m), giving a maximum pressure differential of 0.51 bar.

The seat pitch will be 32" for the all-economy 70 passenger lay-out. The aisle width must be at least 20" (50 cm). The fuselage cross-section has five seats abreast to allow for a stretched version after full development of the 70 passenger version.

Underfloor Luggage Compartment(s)

Underfloor luggage compartment(s) will be used for passenger luggage and freight but do not have to be designed for standard containers.

Performance

Operating Speeds

Maximum cruise Mach number will be M=0.70 at 30000 ft (9120 m) altitude.

Take-off Field Length

At maximum take-off weight the aircraft must be able

to take-off from a 1400 m runway at sea level ISA conditions, according to FAR/JAR 25 rules.

Landing Field Length

At maximum landing weight the landing field length required does not exceed 1200 m. The maximum landing weight can be taken 95% of the maximum take-off weight, because no fuel dumping system is envisaged.

One-Engine-Inoperative Ceiling

The ceiling at maximum take-off weight after engine failure must not be less than 15000 ft (4570 m).

Structure

The structural design might be a fully aluminium-alloy airframe, a fully composite airframe, or a combination of both. A crack-free life of 45000 flights should be possible and an economic repair life of 90000 flights is envisioned for aluminium structures. For fibre-metal laminates a much greater crack-free life and repair life is expected. All primary structural parts should be designed fail-safe and damage tolerant. For the wing CFRP (carbon fibre reinforced plastic) would be an interesting design material for reasons of large stiffness and the possibility of aeroelastic tailoring by finding optimum fibre directions.

Runway Loading

The aircraft should be designed for airfields with runways with a minimum load classification number of LCN=30.

Design of Fuselage and Tail

For the design of the fuselage geometry a CAD program was used, which generates a cross-section and top-view in DXF-format of the cylindrical cabin part for a specified input, such as number of passengers, number of seats abreast, aisle width, aisle height, floor and wall thickness, etc. Two baggage or freight compartments are located underfloor, one in front of and one aft of the main landing gear retraction compartment. The fuselage interior exists of pitch 32" chairs, two galleys, two wardrobes, and two toilets. All space without function has been attempted to eliminate.

To store the retracted main landing gear a bottom fairing is envisioned. The wheel track and wheel base have been calculated by means of stability requirements. The bottom fairing has been sized by making a concept design of the main landing gear.

In figure 1 a cross-section of the aircraft is shown. The fuselage diameter is 3.45 m, 15 cm larger than the diameter

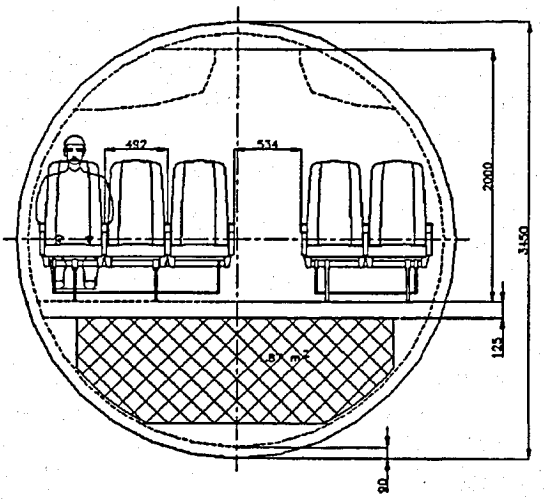

Figure 1: Fuselage cross-section

of the Fokker Jet family to allow some more space between wall and passenger's head. The Avro RJ series has an even larger fuselage diameter of 3.56 m, which should make a high density arrangement with six passengers abreast possible. Since a high density version was not envisaged in the specification a fuselage diameter larger than 3.45 m was not considered.

The fuselage and tail configuration is shown in figure 2 and 3. The reason for choosing a T-tail configuration is the

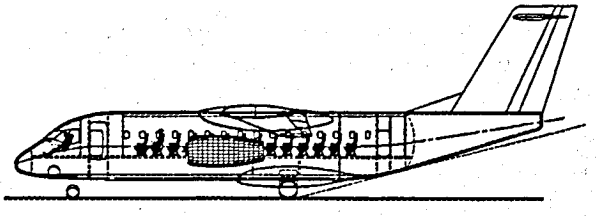

Figure 2: Fuselage side view

wide body fuselage. Due to the small length over diameter ratio compared to aircraft with a four passengers abreast arrangement the actual fuselage length from cockpit to the end of the fuselage cone is relatively small. Using a T-tail configuration helps to extend the arm length between the aerodynamic centre of wing and horizontal tail by about 2 metres. Extending the fuselage length by making an extra freight compartment behind the passenger cabin would allow a cross-tail configuration, however would result in a larger freight space than specified and a large CG-range. A disadvantage of the T-tail is the weight penalty which has to be paid for the larger vertical tail stiffness to prevent flutter. Although a deep stall problem is not anticipated for the present high-wing configuration with wing-mounted engines, windtunnel experiments will be necessary to support a final decision (in case of a real development).

The cockpit windshield was designed to obtain a proper

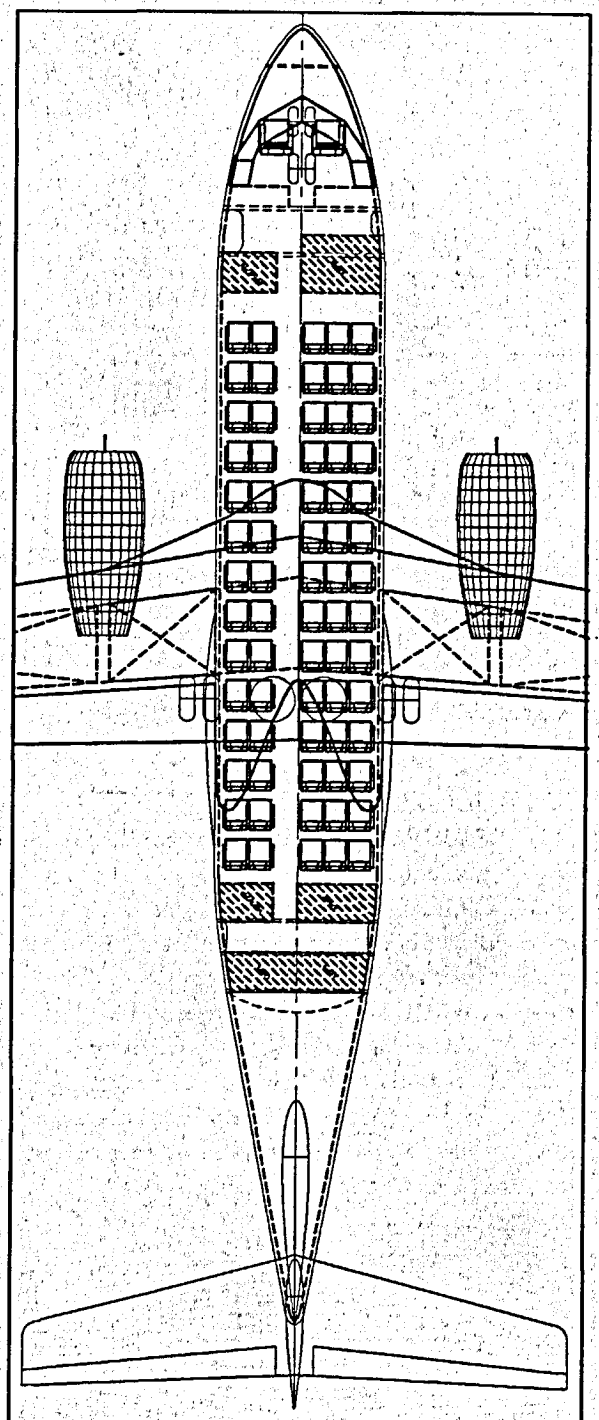

Figure 3: Fuselage top view

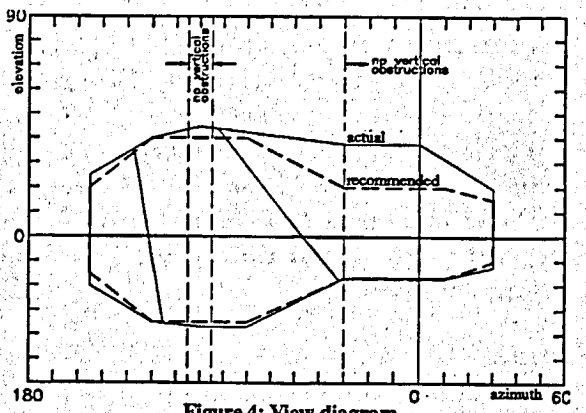

Figure 4: View diagram

view. The view diagram was calculated making a number of iterations to come to the final result. For this purpose the azimuth and elevation angles seen from the eye-point were calculated for several points on the windscreen coaming. The view diagram is plotted in figure 4.

The tailcone was designed to have an upsweep of the bottom line of 17°, to allow for the required take-off rotation freedom of 14°. Further upsweep would not increase the rotation angle, because then a more forward point of the fuselage bottom line would touch the runway. From a panel method calculation with boundary layer coupling no separation problems are expected for small fuselage angles of attack, as can be concluded from figure 5, which shows isobars with gradual C_p variation. In figure 6 the velocity vectors are plotted. The 17° upsweep results in a flat end of the tailcone, which can be seen as an extension of the vertical tail and allows the placement of the auxiliary power unit and fuselage-mounted speedbrakes. The upper line of the tailcone has been kept straight.

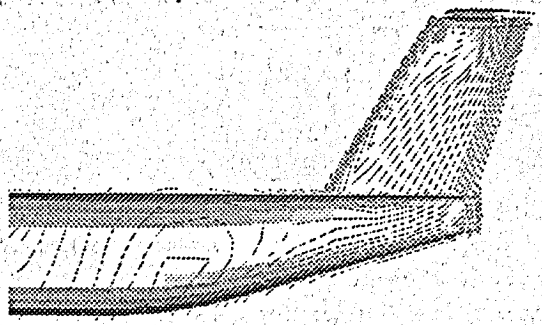

Figure 5: Isobar patern of aft fuselage

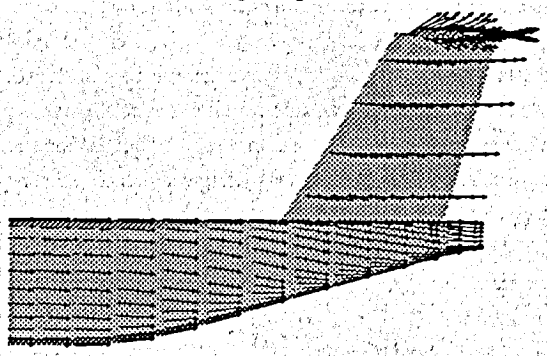

Figure 6: Velocity vectors

A dorsal fin has been proposed in front of the vertical tail (figure 2) to produce vortices along its leading edge which flow over the middle of the rudder under yawing flight conditions. This allows larger yaw-angles and larger

rudder deflections and will increase suction pressure. The maximum lift force generated by the vertical tail is important with respect to a flight condition with one engine inoperative.

The vertical tail area is determined by the following volume coefficient: $V_v = S_v l_v / Sb = 0.08$. For an aspect ratio of 15.5 the largest S_v is obtained. The vertical tail plane design for A=15.5 is therefore used for all other designs. Other parameters are:

taper ratio: $\lambda_v = 0.67$
aspect ratio: $A_v = 1.4$
sweep angle: $\Lambda_{v_{1/4}} = 28°$

The rudder is designed to be double-hinged which allows a rudder relative chord of 35% and a deflection angle of about 35°.

The horizontal tail area is determined by the following volume coefficient: $V_h = S_h l_h / (S\bar{c}) = 1.0$. For an aspect ratio of 8.0 the largest S_h is obtained. The horizontal tail plane design for A=8.0 is therefore used also for the other designs. Other parameters are:

taper ratio: $\lambda_h = 0.5$
aspect ratio: $A_h = 6.0$
sweep angle: $\Lambda_{h_{1/4}} = 12°$

Wing Design

Except for the wing aspect ratio, which varies from 8 to 15.5 by an increment of 1.5, all other wing geometry parameters were fixed. The quarter chord sweep angle has been chosen at 8°, giving an almost straight trailing edge for an aspect ratio of 9.5. It is not necessary to have high wing sweep angle because of the low cruise Mach number of 0.7. In the wing-fuselage junction area, a fairing has been put in front of the wing to reduce relative thickness *t/c* of the root wing section (figure 3). In this way the greater supervelocities, which can be expected in the junction region, are reduced. In figure 7 the six wing designs are depicted. They are generated by the design program to be discussed later.

The fixed wing geometry parameters are:

taper ratio: $\lambda = 0.40$
sweep angle: $\Lambda_{1/4} = 8°$
aileron volume coefficient: $V_{ail} = S_{ail} b_{ail} / Sb = 0.02$
location front wing spar: 20% chord
location aft wing spar: 65% chord

The wingtanks are put outside the structural wing root. In this way tanks in the wing centre-section can be avoided. The tankvolume is calculated according to a constant maximum fuel capacity to be used for the whole family of designs for extended range flights with approximately half of the total number of passengers. It is noted from figure 7 that the high aspect ratio wings tend to become volume-limited.

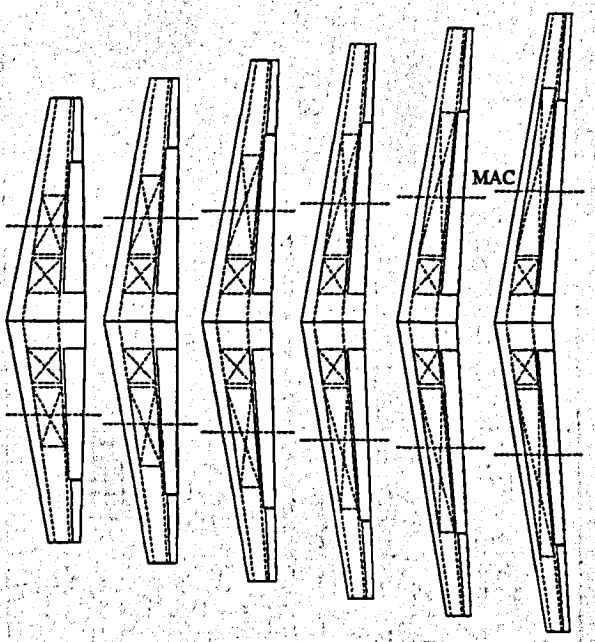

Figure 7: Wing designs for 6 aspect ratios

Turbofan Engine

A UDF (UnDucted Fan), ADF (Advanced Ducted Fan) or high bypass turbofan engine was proposed as means of propulsion. A high bypass turbofan engine was chosen, since engine data of other engines were lacking. Even data of a high bypass turbofan were difficult to acquire. Initially the (outdated) Rolls Royce RB410 (project) with a bypass ratio of 9.8 was used in this study, which was later replaced by data of the BMW-Rolls Royce BR512 project engine with a bypass ratio of 5. The data used for this study are presented in figures 8 and 9 showing engine geometry and thrust lapse curves for three engine ratings.

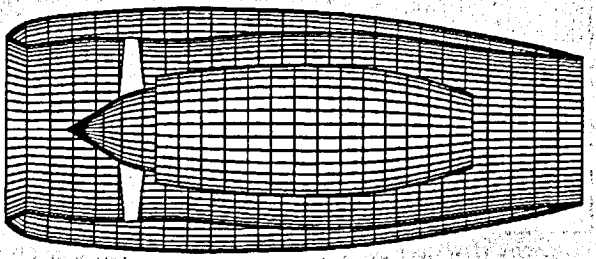

Figure 8: BR512 engine-nacelle geometry

Further turbofan data of the BR512 are listed below:

average specific fuel consumption: $C_T / \sqrt{\theta} = 0.61 N/h/N$
take-off $\dot{m}$ at S/L: $\dot{m} = 204 kg/s$
bypass ratio in design point: $\lambda = 5$
intake diameter: $d_{int} = 1.22m$

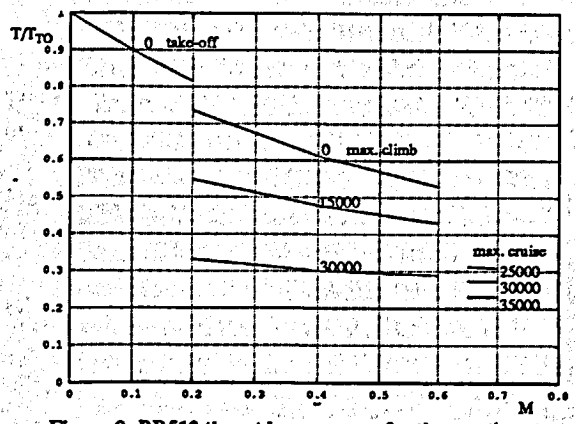

Figure 9: BR512 thrust lapse curves for three ratings

ADAS design and analysis program

In figure 10 the design and analysis program is visualized in a flow diagram. The program first selects an aspect

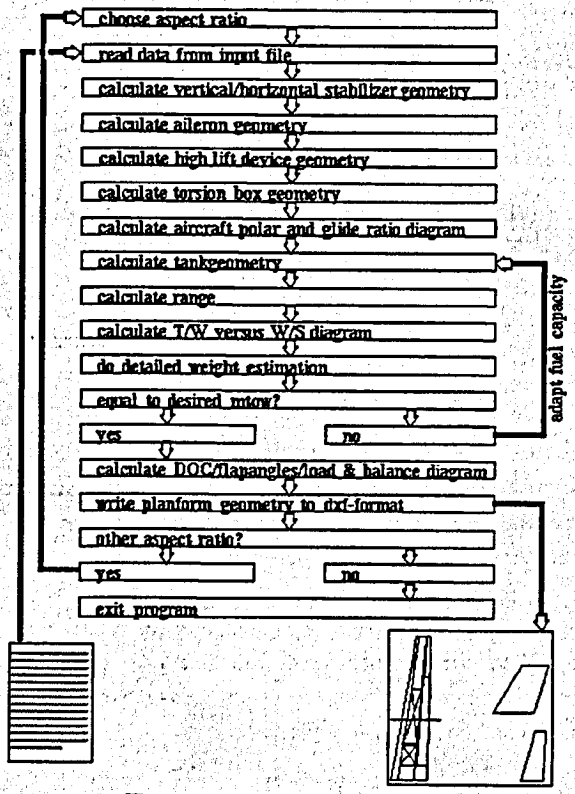

Figure 10: Flow diagram of ADAP

ratio A. Successively the input data are read from a standard input file. In this file data like thrust lapse rates, atmospheric properties, aircraft architecture, aircraft requirements, initial values for S and W_{TO} and drawing specifications are listed. Initial configuration choices (the aircraft architecture), like T-tail and high-wing position, are laid down in a parametric geometrical format by means of mathematical relations. The aircraft parametric architecture is shown in figure 11.

Before the remaining of the flow diagram is discussed,

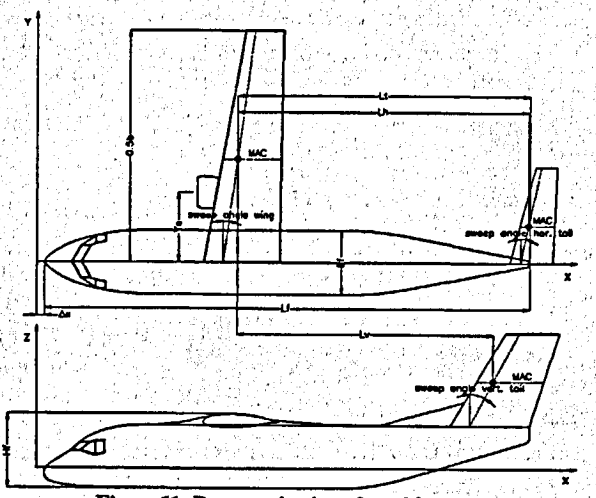

Figure 11: Parametric aircraft architecture

first the aircraft requirements will be considered. These are: landing distance, *BFL*, take-off distance, cruise Mach number M_c for two altitudes, second segment climb and ceiling with one engine inoperative. Some of these requirements are derived or stated below:

Cruise:

Two cruise conditions will be considered, both for M=0.7, but for different altitudes: 30000 ft and 35000 ft. For cruise condition the following equilibrium equations hold:

$$T = D = C_D \frac{1}{2} \gamma p M^2 S \qquad (1)$$

$$W = L = C_L \frac{1}{2} \gamma p M^2 S \qquad (2)$$

or:

$$C_L = \frac{W/S}{\frac{1}{2}\gamma p M^2} \qquad (3)$$

The aircraft polar for cruise configuration is given by:

$$C_D = C_{D_0} + \frac{C_L^2}{\pi A e} \qquad (4)$$

Substituting eq. (3) for C_L into eq. (4) and subsequently substituting the obtained expression for C_D into eq. (1) gives the following expression for the thrust to weight ratio in cruise condition:

$$\frac{T}{W} = \frac{\frac{1}{2}\gamma p M^2 C_{D_0}}{W/S} + \frac{W/S}{\frac{1}{2}\gamma p M^2 \pi A e} \qquad (5)$$

We want to express the thrust to weight ratio in terms of the

take-off thrust and take-off weight, because those are determining the engine choice. For this reason we write:

$$\frac{T}{W} = \frac{T_{TO}}{W_{TO}} \frac{T}{T_{TO}} \frac{W_{TO}}{W} \tag{6}$$

Substituting eq. (6) into eq. (5) we can write:

$$\frac{T_{TO}}{W_{TO}} = \frac{W/W_{TO}}{T/T_{TO}} \left(\frac{\frac{1}{2}\gamma p M^2 C_{D_0}}{W/S} + \frac{W/S}{\frac{1}{2}\gamma p M^2 \pi A e} \right) \tag{7}$$

This equation can be refined further by substituting all contributions to C_{D_0}. Here it is important to notify that W/W_{TO} has been assumed equal to 1, and T/T_{TO} was read from the BMW-Rolls Royce BR-512 brochure for the two altitudes mentioned. For M=0.7 at 30000 ft the thrust ratio is 0.27 and for M=0.7 at 35000 ft it was found to be 0.23 (figure 9).

Ceiling with one engine inoperative:

Assuming a flight condition for minimum drag at $(L/D)_{max}$, one can derive:

$$\frac{N_e - 1}{N_e} \frac{T}{W} = 2\sqrt{\frac{C_{D_0}}{\pi A e}} + \frac{C}{\sqrt{2RT_0}} \frac{\sqrt[4]{C_{D_0} \pi A e}}{\sqrt{W/S \frac{\theta}{p}}} \tag{8}$$

If we define the ceiling as the altitude at which C=0.5 m/s and furthermore substitute R=287.05 m^2/s^2, T_0=288.15 K and eq. (6), we obtain:

$$\frac{T_{TO}}{W_{TO}} = \frac{N_e}{N_e - 1} \frac{W/W_{TO}}{T/T_{TO}} \times \left(2\sqrt{\frac{C_{D_0}}{\pi A e}} + \frac{0.00123}{\sqrt{\theta}} \frac{\sqrt[4]{C_{D_0} \pi A e}}{\sqrt{W/S \frac{1}{p}}} \right) \tag{9}$$

Again W/W_{TO} has been assumed equal to 1. For this flight condition T/T_{TO}=0.48, for $M \approx 0.4$ at 15000 ft altitude.

Take-off distance:

The required wing loading for an all-engines take-off with a specified take-off distance can be found from:

$$\frac{W_{TO}}{S} = \left\{ \frac{S_{TO}}{f_{TO}} - \frac{h_{TO}}{\gamma_{LOF}} \right\} \times \frac{\rho g C_{L_{max}} (1 + \gamma_{LOF}\sqrt{2})}{(V_3/V_s)^2 \left\{ (\bar{T}/W_{TO} - \mu^1)^{-1} + \sqrt{2} \right\}} \tag{10}$$

In this equation f_{TO} is a safety factor for the take-off distance and equals 1.15 according to FAR-25. The screen height h_{TO}=10.7 m and the ratio between speed at screen height and stall speed V_3/V_s is taken 1.3. The mean thrust to weight ratio during the take-off run can be related to the static take-off thrust to weight ratio (M=0) by using statistical data, yielding:

$$\frac{\bar{T}}{W_{TO}} = 0.75 \frac{5 + \lambda}{4 + \lambda} \frac{T_{TO}}{W_{TO}} \tag{11}$$

Further we may assume for the equivalent friction coefficient and lift-off angle of climb:

$$\mu^1 = 0.01 C_{L_{max}} \tag{12}$$

$$\gamma_{LOF} = 0.9 \frac{\bar{T}}{W_{TO}} - \frac{0.3}{\sqrt{A}} \tag{13}$$

Landing distance:

The landing distance requirement for the wing loading can be found from the following statistical formula for given landing distance:

$$\frac{W_{TO}}{S} = \frac{1}{W_{land}/W_{TO}} \left(\frac{S_{land}}{f_{land} h_{land}} - 10 \right) \times \frac{h_{land} \rho g C_{L_{max}}}{\frac{1.52}{\bar{a}/g} + 1.69} \tag{14}$$

According to FAR Part 91 a safety factor f_{land}=5/3 has to be used. The screen height for landing h_{land}=15.3 m. The deceleration $\bar{a}/g$ has been taken 0.47, which means nose wheel braking is not applied (cheaper).

Second segment climb (one engine inoperative):

The second segment climb path is a 2.4% climb performed after rotation with one engine inoperative. For this climb condition we can derive:

$$\frac{N_e - 1}{N_e} \frac{T}{W_{TO}} - \frac{D}{L} = \gamma_2 \tag{15}$$

Using eq. (6) one can write eq. (15) as follows:

$$\frac{T_{TO}}{W_{TO}} = \frac{W/W_{TO}}{\frac{N_e - 1}{N_e} \frac{T}{T_{TO}}} \left(0.024 + \frac{C_D}{C_L} \right) \tag{16}$$

Also for this case W/W_{TO} has been assumed equal to 1. Assuming the climb occurs at $V_2 = 1.2V_s$ and assuming on forehand $C_{L_{max}}$=2.4 for flaps in take-off position, we can

calculate: C_{L_2}=1.67, V_2≈60.9 m/s (W_{TO}/S = 3800 N/m^2), M_2≈0.18. For zero altitude and M_2≈0.18 we find from the engine brochure (or from eq. (11)) the following thrust ratio:

$$\frac{T_2}{T_{TO}} = 0.83$$

For the drag coefficient in the second segment climb where flaps are in take-off position the following empirical formula can be used:

$$C_{D_2} = C_0 + \frac{(C_{L_2})^2}{\pi AE} \qquad (17)$$

In this equation the equivalent zero-lift drag coefficient C_0=.005 and the equivalent Oswald factor for flaps down is E=0.61.

Balanced field length:

The required wing loading to satisfy the prescribed *BFL* can be calculated from:

$$\frac{W_{TO}}{S} = \rho g C_{L_2} \times \left\{ \frac{1.159\,(BFL - \Delta S_{TO})\,(1 + 2.3\Delta\gamma_2)}{(\bar{T}/W_{TO} - \mu^1)^{-1} + 2.7} - h_{TO} \right\} \qquad (18)$$

In eq. (18) $\Delta\gamma_2$ is the difference between the second segment climb gradient γ_2 according to eq. (15) and the minimum value of γ_2 permitted by the airworthiness regulations (2.4%). It can therefore be written as:

$$\Delta\gamma_2 = \gamma_2 - 0.024 \qquad (19)$$

Furthermore the inertia distance ΔS_{TO} can be assumed equal to 200 m.

Having considered the aircraft requirements, the explanation of the flow diagram as depicted in figure 10 will be proceeded. After reading the input file, vertical and horizontal stabilizer geometry are calculated according to the previously specified volume coefficients. Also aileron and high lift device surfaces are calculated and positioned in the wing planform. Then the torsionbox geometry is determined for the previously specified spar locations.

Successively the aircraft polar and glide ratio diagram are calculated for an assumed choice of wing area *S*. In figure 12 the aircraft polar is shown for various aspect ratios for a fixed wing area *S*. The zero lift aircraft drag C_{D_0}=0.02.

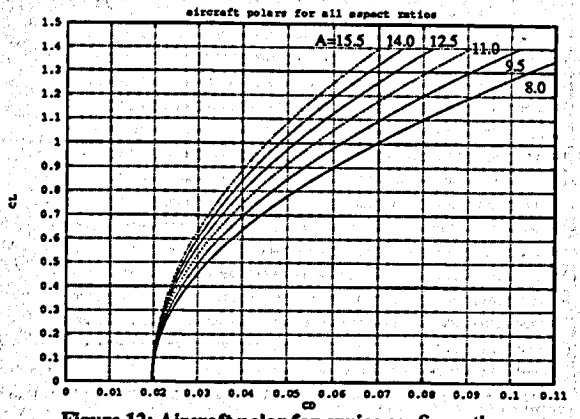

Figure 12: Aircraft polar for cruise configuration

The induced drag reduces for increasing aspect ratio inversely proportional to A ($C_{D_i} = C_L^2/\pi Ae$). In figure 13

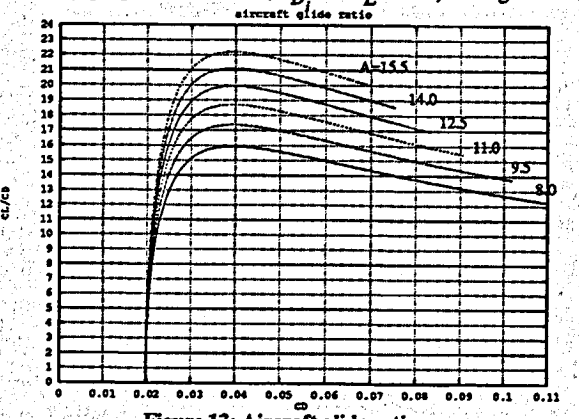

Figure 13: Aircraft glide ratio

the glide ratio diagram is plotted. The maximum glide ratio *L/D* equals approximately 16 for A=8 and 22 for A=15.5.

Having calculated the drag polar, a calculation can be performed to determine the fuel capacity and related tank volume. For the baseline design (A=11) the fuel capacity was chosen such that the harmonic range was 2500 km. This requirement determined the W_{TO}, which was held constant for all other designs. In the first iteration step of the loop (figure 10) an initial small amount of fuel is taken, which converges in a few steps to:

$$W_F = W_{TO} - W_{OE} - W_P \qquad (20)$$

With this amount of fuel the harmonic range can be calculated, which is different for the various designs. Only the baseline design will have the specified range of 2500 km. The tank volume, however, is not based on the amount of fuel calculated by eq. (20), but is based on a constant maximum fuel capacity for all designs for an extended range with less passengers. The number of passengers for a flight with extended range will therefore vary for the different designs. This is shown in table 1. It should be clear that for the harmonic range, which is important for this design study, the tanks are not completely filled.

aspect ratio	number of passengers.	maximum range
8	45	4298
9.5	41	4535
11	36	4720
12.5	31	4869
14	26	4992
15.5	22	5096

Table 1: Maximum range for constant max. fuel volume

In the loop shown in figure 10 also an aircraft sizing diagram (T_{TO}/W_{TO} versus W_{TO}/S) is calculated according to eqs. (1) through (19). Next a detailed weight estimation is done as last part in the loop. In the first iteration step the W_{ZF} is calculated, which finally converges to the specified W_{TO}, by adding fuel according to eq. (20).

After convergence to the specified W_{TO}, calculations are performed to control flap feasibility and high-wing longitudinal position. The wing position should be such that a feasible CG range is obtained. To control flap feasibility $C_{L_{max}}$ is calculated for the clean wing. Then it is checked whether the flaps can generate the requested $C_{L_{max}}$ for the landing. To control the wing position a load and balance diagram is calculated which can be visualized during the design process. Two load and balance diagrams are plotted in figures 13 and 14. From these diagrams the CG range can

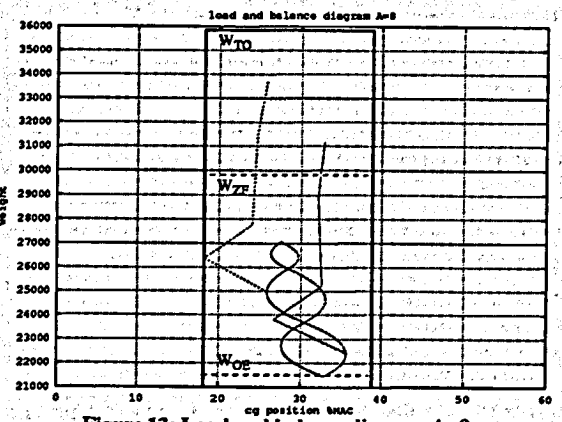

Figure 13: Load and balance diagram A=8

be read off. To obtain the smallest trim drag the aft CG position should lay as far aft as possible. In this way the smallest negative tail loads will result and as a consequence the smallest trim drag is obtained. The aft boundary in figures 13 and 14 implies a loading restriction, which in case of A=15.5 means to first load the forward baggage/freight compartment before loading the aft one. The wing position, more specifically the wing AC, could be held at the same

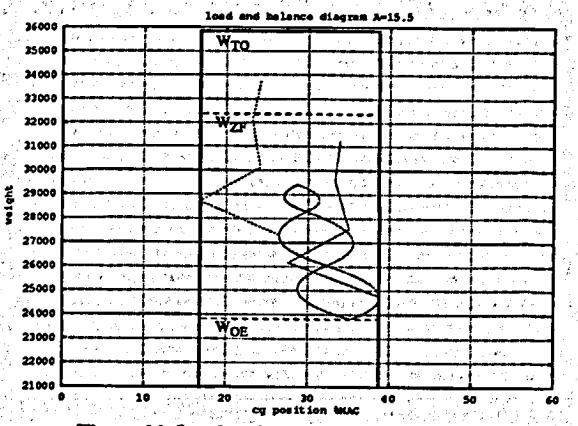

Figure 14: Load and balance diagram A=15.5

longitudinal position for the whole family of aircraft.

The last step in the ADAP is to write the planform design to a DXF-file which can be imported into a CAD program. Such a planform design is shown in figure 15.

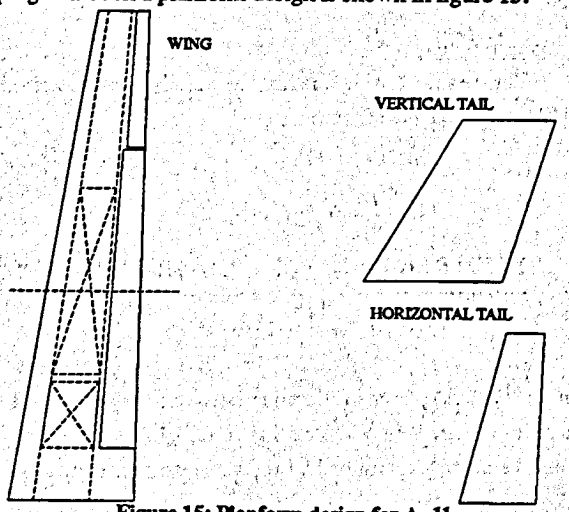

Figure 15: Planform design for A=11

Subsequently the whole program can be run for other aspect ratios, which is in fact automatized.

Aircraft sizing diagrams

In the previous chapter the performance requirements were discussed and formulated. In this chapter the actual aircraft sizing diagrams, which reflect these requirements, will be given for the smallest and largest aspect ratio. In figure 16 and 17 (page 11) two sizing diagrams are plotted for A=8 and A=15.5 respectively. A $C_{L_{max}}$ of 2.4 for take-off and 2.9 for the landing have been taken as the maximum values to be used. For the design with A=8 the feasible design space is limited by four different constraints, which are:

-cruise, M=0.7, FL 30000 ft ISA

-combination of second segment climb requirements and *BFL*

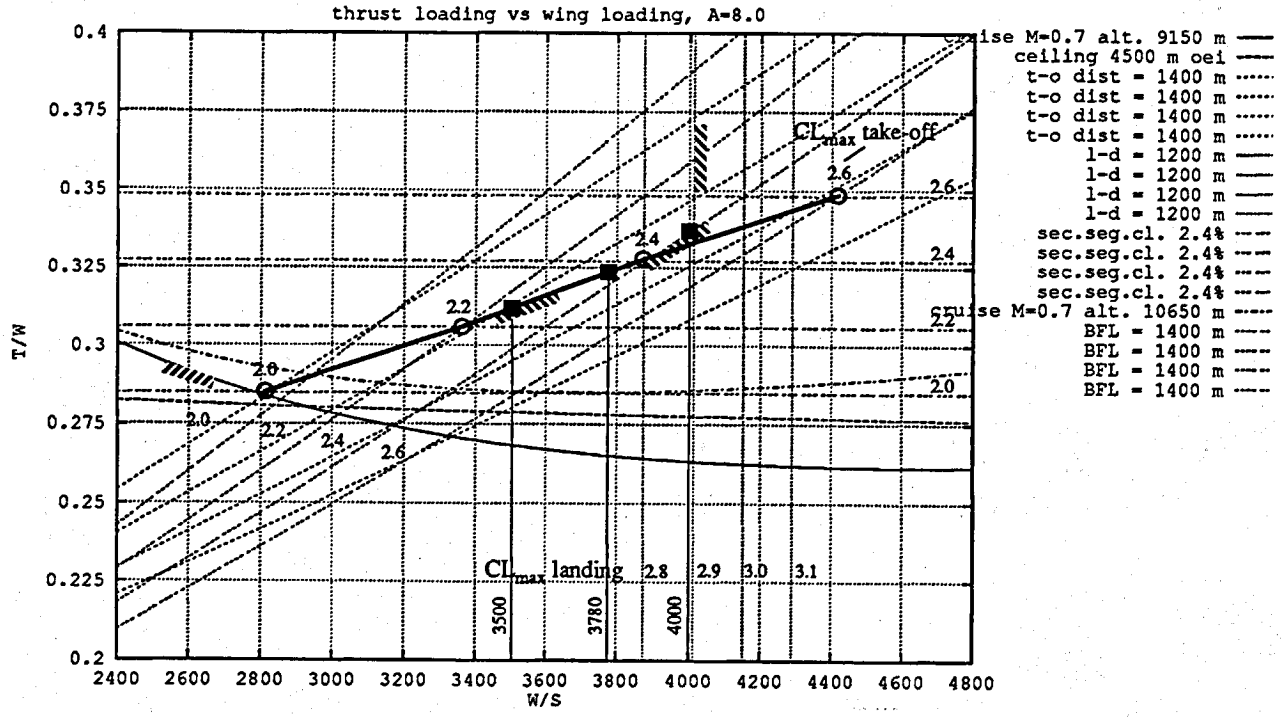

Figure 16: Thrust to weight ratio versus wing loading diagram A=8.0

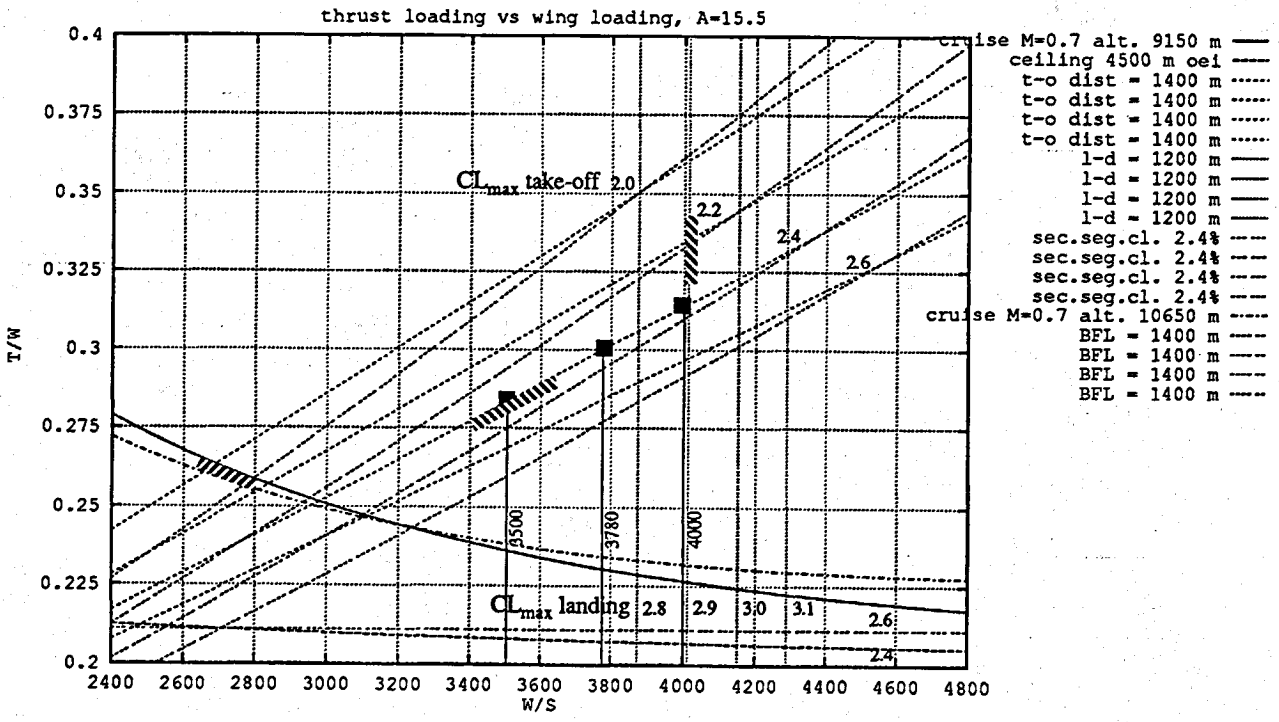

Figure 17: Thrust to weight ratio versus wing loading diagram A=15.5

-*BFL* requirement for $C_{L_{max}}$=2.4 during take-off
-landing distance for $C_{L_{max}}$=2.9 in landing
For the design with A=15.5 the feasible design space is limited by three different constraints, which are:
-cruise, M=0.7, FL 30000 ft ISA
-take-off distance requirement
-landing distance for $C_{L_{max}}$=2.9 in landing

For three values of W_{TO}/S design points were chosen for each aspect ratio A resulting in 6x3=18 different design points. In this way a parametric study could be performed with W_{TO}/S and A as independent variables. In figure 18 the chosen points are shown in a carpet plot.

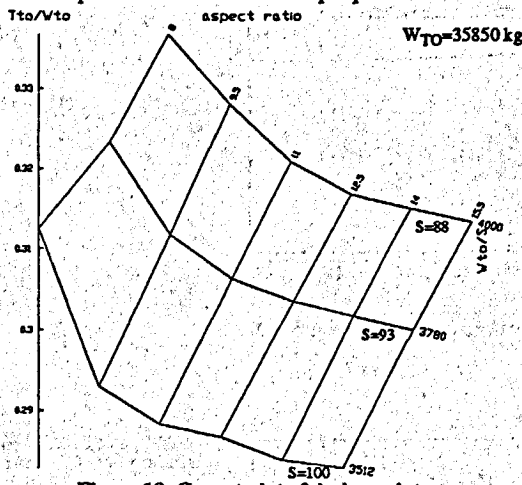

Figure 18: Carpet plot of design points

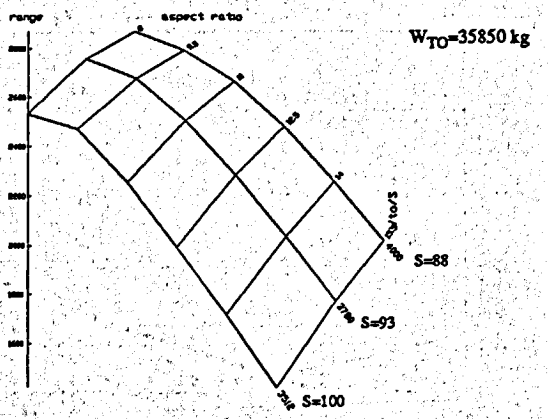

Figure 19: Range as function of W_{TO}/S and A

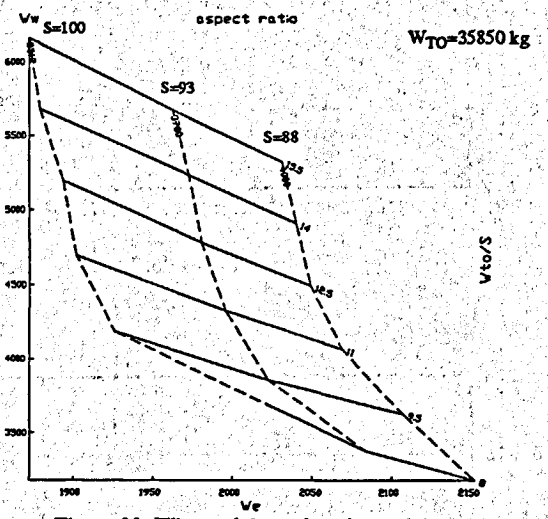

Figure 20: Wing weight and engine weight

Parametric Survey

In this chapter the design points indicated in figure 18 will be analysed with respect to four dependent variables, which are harmonic range R, wing weight W_w, engine weight W_e and DOC. Here it is important to observe that the study has been performed for constant W_{TO}. Under this restriction a maximum range might be found for a certain optimum aspect ratio A for each wing loading. The range is plotted in figure 19 and one can observe no real optimum is present. Consider the following formula for the range:

$$R \cong \frac{a_0 ML/D}{C_T/\sqrt{\theta}} ln \frac{1}{1 - W_F/W_{TO}} \qquad (21)$$

Two variables determine the range, which are glide ratio and fuel ratio. Apparently the increase of glide ratio cannot win from the decrease of fuel weight for increasing aspect ratio.

In figure 20 a carpet plot is shown of wing weight W_w and engine weight W_e as function of wing loading and aspect ratio. The reason for the tendency to a maximum range for the two smaller wing surface areas S, becomes clear in this figure. Increasing with aspect ratio from A=8 to 9.5, the engine weight decreases significantly in comparison to the increment of wing weight. For S=88 the reduction in engine weight is much smaller. For aspect ratios larger than 9.5 the reduction in engine weight is not significant while the wing structural weight keeps increasing. The smallest total weight increase (W_w + W_e) due to aspect ratio enlargement is obtained for S=100 and S=93 when the aspect ratio is increased from A=8 to A=9.5. Consequently the decrease in fuel weight will be the smallest when moving from A=8 to A=9.5. In this region a tendency to a maximum range is therefore visible, because the increase in L/D tends to win from the decrease in fuel weight in eq. (21).

Finally the DOC will be estimated for all design points. This is done by deriving a formula for DOC per pax-km based on statistical data of comparable aircraft. For the derivation of DOC per pax-km the following formula is used giving the DOC over the aircraft's lifetime:

$$DOC = C_f + C_m + C_s \qquad (22)$$

DOC consists of three costs components: costs associated

with flying operations C_f, direct maintenance costs C_m and standing costs of flight equipment C_s. C_f can be written as:

$$C_f = DU\left(c_{fc} + a\frac{W_F}{t_b}\right) \tag{23}$$

The maintenance costs can be written as:

$$C_m = DU\left(\frac{c_{m_t}}{t_b}\right) \tag{24}$$

The standing costs of flight equipment are assumed to be equal for the whole family of designs. The following formula for DOC per pax-km could be derived using eqs. (22) through (24):

$$DOC_{pax-km} = \frac{DOC}{DUV_b N_{pax}} = \frac{aW_F + c_{m_t}}{RN_{pax}} + \frac{c_{fc}}{V_b N_{pax}} + \frac{C_s}{DUV_b N_{pax}} \tag{25}$$

The DOC per pax-km could be expressed as function of fuel weight and range using statistical data of comparable aircraft, a=\$0.344/kg, c_{m_t}=\$373/cycle, D=30 years, U=(90000/D)t_b=4500t_b, c_{f_c}=\$1.4E6/U, C_s=180.4E6, yielding:

$$DOC_{pax-km} = \frac{1}{N_{pax}}\left(\frac{0.344W_F}{gR} + \frac{2020}{R}\right) \tag{26}$$

In the figure 21 a carpet plot is shown of this expression

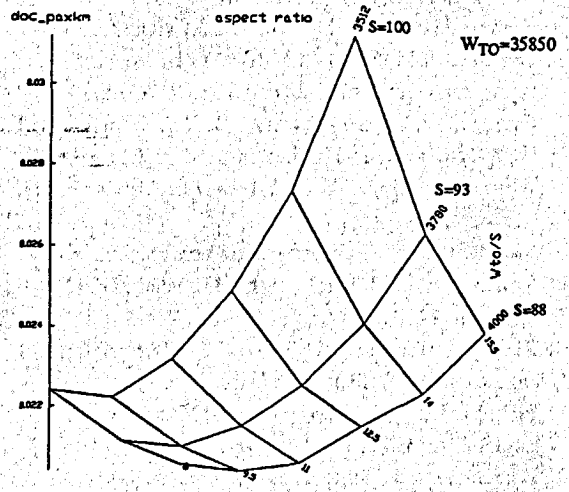

Figure 21: Parametric survey of DOC per paxkm

for the 18 design points (N_{pax}=const=70). It can be concluded the optimum aspect ratio for minimum DOC per pax-km does not coincide with the optimum aspect ratio for maximum range. For all wing areas, minimum DOC is obtained for A=9.5, while maximum range is obtained for an aspect ratio A=8 within the aspect ratio bounds of this study.

Having performed this parametric survey, a final choice of wing loading W_{TO}/S or wing gross area S has to be made for the complete family of designs. From figures 19 and 21 it was observed that a larger range and smaller DOC per pax-km might be obtained for higher wing loading (smaller S). Unfortunately an extremely unbalanced design (big engines!) is obtained for the highest wing loading (especially for greater aspect ratios), see figures 16 and 17. This could be improved by increasing the $C_{L_{max}}$ for take-off to a maximum of 2.6 and by increasing the cruise Mach number. In this study, however, $C_{L_{max}}$ for take-off was limited to 2.4 and according to the proposal M_c was chosen equal to the maximum of 0.7. For these reasons a wing loading of 3780 N/m^2 (S=93 m^2) was chosen giving a more balanced design with convenient range performance and DOC. Another possibility to decrease the gap between the take-off and cruise required T_{TO}/W_{TO} would be to increase the cruise altitude. Within the bounds of the specification the cruise altitude might be enlarged to 35000 ft for the design family (see figures 16 and 17) resulting in a maximum cabin pressure differential of 0.51 bar.

For the chosen wing loading of 3780 N/m^2 (S=93 m^2) the data for the various designs can be tabulated as done in table 2. The design with A=8 is dominated by the combination of the second segment climb and balanced field length requirements. All other designs are dominated by the take-off distance requirement, and therefore have a nearly constant thrust to weight ratio. Minimum DOC per pax-km is obtained by the design with A=9.5, indicated by thick lines in table 2. The maximum range is reached for A=8, the boundary of the aspect ratio domain.

A	$\frac{T_{TO}}{W_{TO}}$	$T_{TO}/2$ [kN]	R [km]	DOC [\$/ pax-km]
8	0.3233	56.9	2758	2.114E-2
9.5	0.3117	54.8	2677	2.101E-2
11	0.306	53.9	2506	2.153E-2
12.5	0.304	53.4	2288	2.254E-2
14	0.302	53.1	2039	2.409E-2
15.5	0.300	52.8	1777	2.631E-2

Table 2: Design data for various designs with S=93

Finally a three dimensional drawing of the baseline design with A=11 (without fairings and engine pylons) is shown in figure 22.

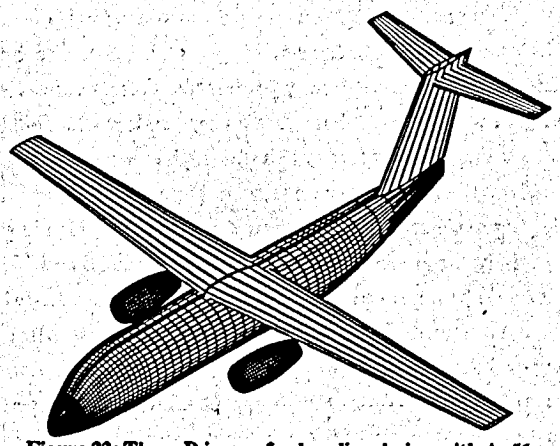

Figure 22: Three-D image for baseline design with A=11

Weight breakdown and weight aspects

For the baseline design a weight breakdown is given in appendix 2. Based on this weight breakdown and similar weight breakdowns for the other designs, in this chapter the main aircraft weight components as function of aspect ratio will be analysed. For this purpose consider figure 23. The

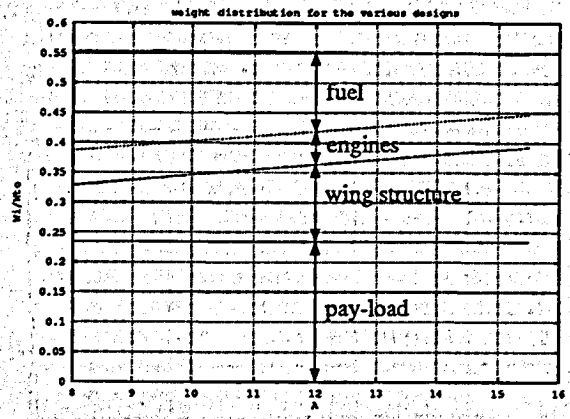

Figure 23: Sensitivity of weight components to aspect ratio

pay-load is a constant fraction of the take-off weight, approximately 23.4%. The weight of wing structure increases linearly with aspect ratio. Engine weight does not vary significantly, see also table 2. Subtracting the weight contribution of fuselage, tail, crew, aircraft systems etc. from W_{TO} yields a nearly constant weight fraction of 55%. A small variation exists due to decreasing weight of nacelles and thrust reversers with decreasing engine thrust. As a result of the previous statements fuel weight has to decrease approximately with the same amount as wing weight increases.

Conclusions

A 70 passenger airliner has been designed for 6 different aspect ratios for constant W_{TO}. Cruise Mach number equals 0.7 and the cruise altitude is 30000 ft. Cruise altitude can even be higher up to 35000 ft, the service ceiling constrained by maximum cabin pressure differential. The aircraft is propelled by two fuel-efficient and light-weight BMW-Rolls Royce BR512 project engines. The wing loading was varied by choosing three values for the gross wing area S. Finally S was chosen equal to 93 m^2, giving balanced designs with moderate thrust, good range performance and low *DOC* for the various aspect ratios. The design with A=8 is dominated by the combination of second segment climb and balanced field length requirements. All other designs are dominated by the take-off field length requirement for $C_{L_{max}}$=2.4.

Different optimum aspect ratios were found for maximum range and minimum *DOC*, A=8 and A=9.5 respectively.

References

[1] Torenbeek E., Proposal for Multidisciplinary wing optimization study, Delft, January 1995.

[2] Torenbeek E., Synthesis of Subsonic Airplane Design, Delft, 1988.

[3] Torenbeek E., Introduction to Preliminary Aircraft Design, Volume 2, Advanced course on subsonic and supersonic design optimization, Delft, April 1988.

[4] Bil C., Aircraft Design and Analysis System (ADAS), users manual, Delft, February 1995.

[5] Jane's All the World's aircraft 1994-1995.

[6] Roskam J., Airplane Design, Part 2, Wichita, 1988.

[7] Brochure of M45S-11 (RB410-11) variable pitch geared turbofan, Rolls Royce / SNECMA, June 1973.

[8] Greff E., Becker K., Karwin M., Rill S., Integration of High By-pass Ratio Engines on Modern Transonic Wings for Regional Aircraft, Deutsche Airbus GmbH, Bremen, 1991.

[9] Kappler G., Die neue Generation von Flugantrieben für den Zivilen Flugverkehr, TU München, DGLR Jahrbuch, 1988.

[10] Richter H., Performance data of BR-512 turbofan engine, BMW-Rolls Royce, Dahlewitz, 1995.

[11] Friend C.H., Aircraft Maintenance Management, England, April 1992.

[12] Baaren van R.J., Smit K., Economic Aspects of Air-Transportation (Luchttransportkunde), Delft, Januari 1995.

Appendices

Appendix 1: Thrust to weight ratio versus wing loading diagrams.

Appendix 2: Weight breakdown for design with A=11.

Appendix 3: Three-view drawing of baseline design

Appendix 1: Thrust to weight ratio versus wing loading diagrams

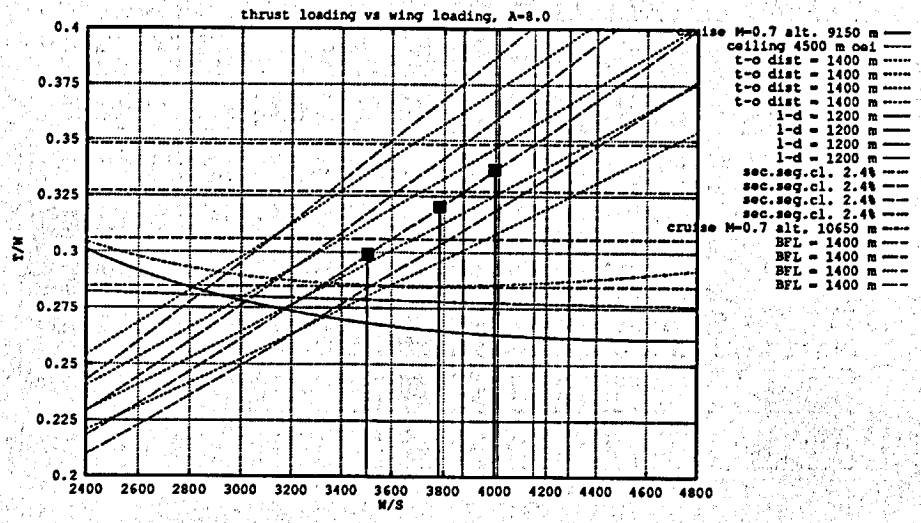

Fig. A1: Thrust to weight ratio versus wing loading diagram A=8

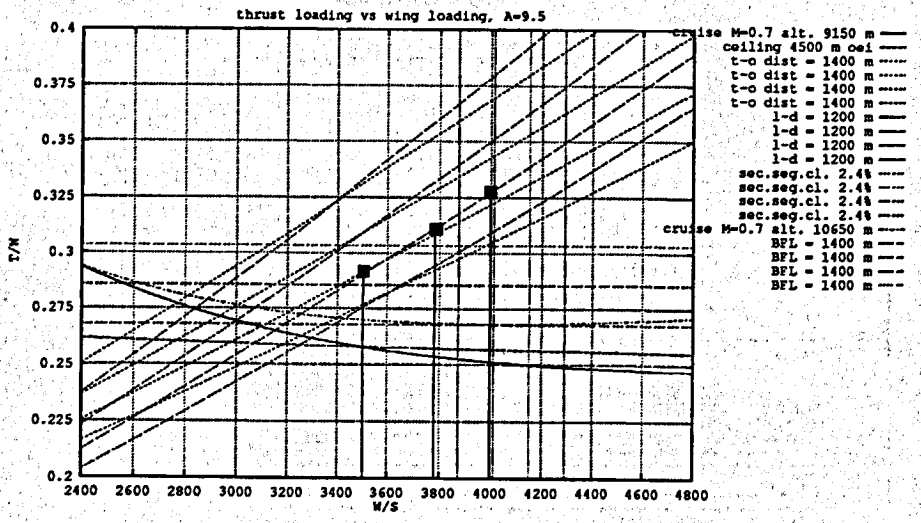

Fig. A2: Thrust to weight ratio versus wing loading diagrams A=9.5

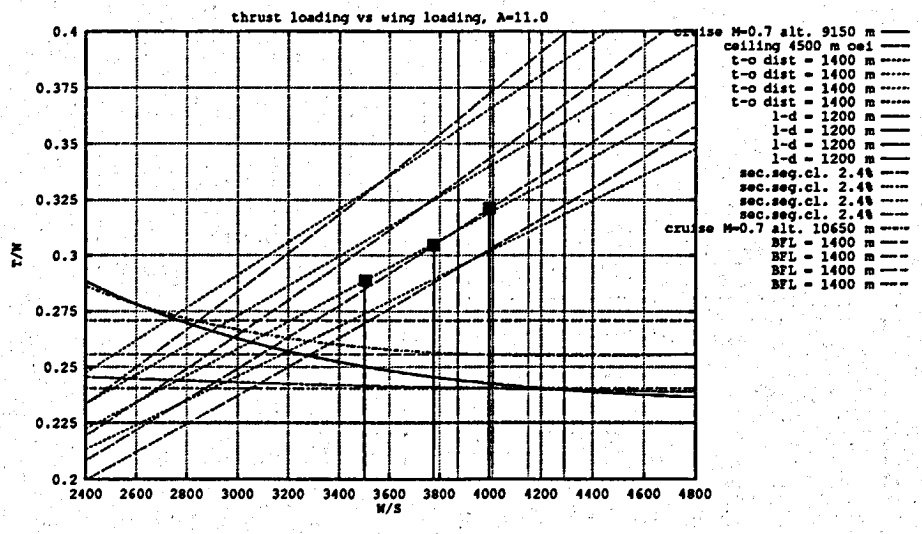

Fig. A3: Thrust to weight ratio versus wing loading diagrams A=12.5

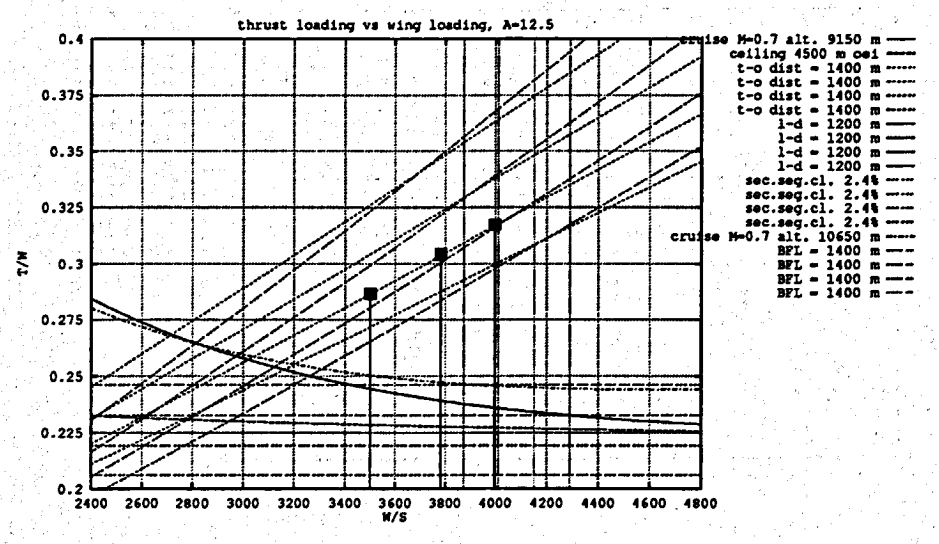

Fig. A4: Thrust to weight ratio versus wing loading diagrams A=12.5

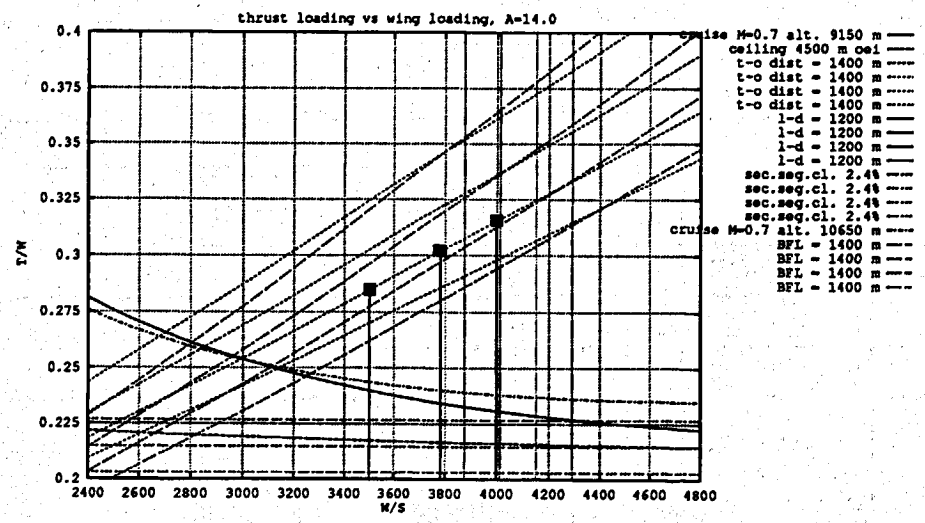

Fig. A5: Thrust to weight ratio versus wing loading diagram A=14.0

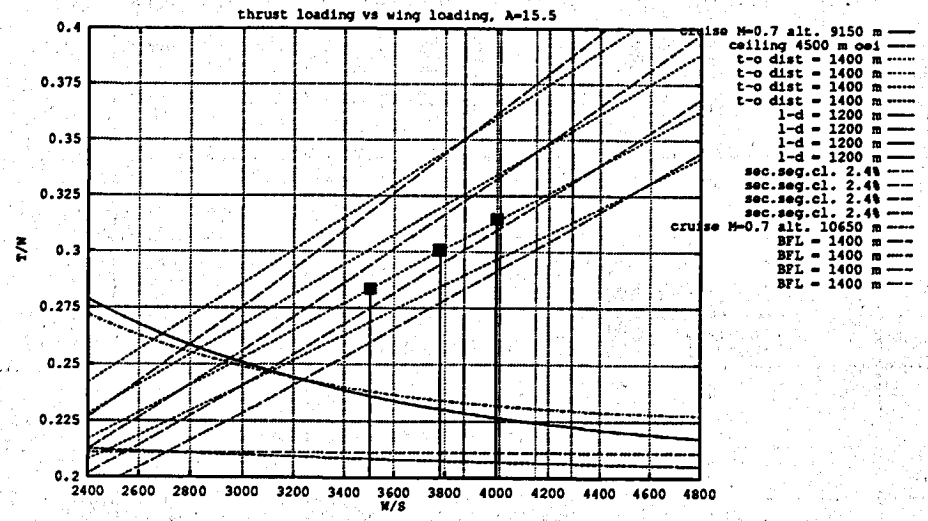

Fig A6: Thrust to weight ratio versus wing loading diagram A=15.5

Appendix 2: Weight breakdown for design with A=11.0

PARTITION NAME	MASS [kg]	MASS/MTOW × 100%	Xcg [mm]	Ycg [mm]	Zcg [mm]
port wing half	2162.82	6.03296	14661.9	-6396.9	2566.6
starboard wing half	2162.82	6.03296	14661.9	6396.9	2566.6
horizontal tail	121.69	0.33945	27430.3	-2062.6	7363.4
horizontal tail	121.69	0.33945	27430.3	2062.6	7363.4
vertical tail	274.26	0.76502	25973.1	0.0	4597.9
fuselage	3528.69	9.84293	12384.5	0.0	617.9
port main land-inggear	643.64	1.79536	12554.6	-1725.5	-1107.6
starboard main landinggear	643.64	1.79536	12554.6	1725.5	-1107.6
nose land-inggear	262.33	0.73175	1788.7	0.0	-605.7
controls group	267.20	0.74533	14397.6	-6853.8	2343.4
controls group	267.20	0.74533	14397.6	6853.8	2343.4
port nacelle	615.37	1.71652	11202.3	-4797.7	352.6
starboard nacelle	615.37	1.71652	11202.3	4797.7	352.6
port bare dry engine	998.12	2.78417	11202.3	-4797.7	352.6
starboard bare dry engine	998.12	2.78417	11202.3	4797.7	352.6
port fuel system	91.74	0.25590	12781.7	-1075.0	2625.3
starboard fuel system	91.74	0.25590	12781.7	-1075.0	2625.3
thrust reversers	179.66	0.50115	12793.3	-4797.7	959.4
thrust reversers	179.66	0.50115	12793.3	-4797.7	959.4
auxiliary power unit	143.40	0.40000	25588.6	0.0	1739.5
instr. & nav. equipment	239.99	0.66943	1886.2	0.0	601.9
hydr. & pneu. group	2743.11	7.65163	15048.4	0.0	617.9
electrical group	1352.75	3.77336	15048.4	0.0	617.9

PARTITION NAME	MASS [kg]	MASS/MTOW × 100%	Xcg [mm]	Ycg [mm]	Zcg [mm]
flight deck accessories	56.95	0.15885	3110.5	0.0	908.7
floor covering	115.60	0.32246	12682.0	0.0	125.0
insulation/wall covering	838.62	2.33924	12682.0	0.0	617.9
cargo restr. cargo comp.1	26.50	0.07391	7785.4	0.0	-447.2
cargo restr. cargo comp.2	12.03	0.03356	16761.2	0.0	-447.2
fixed oxygen systems	94.40	0.26332	12452.8	0.0	1666.5
anti-fire provisions	43.02	0.12000	12682.0	0.0	617.9
escape provisions	31.71	0.08845	12452.8	0.0	44.3
galley front	124.74	0.34795	5350.0	830.0	1030.0
galley aft	102.06	0.28469	18380.0	790.0	1030.0
toilet port side	136.00	0.37936	19830.0	-910.0	820.0
toilet starboard	136.00	0.37936	19830.0	910.0	820.0
wardrobe front	15.00	0.04184	5540.0	-1070.0	1030.0
wardrobe aft	15.00	0.04184	18384.3	-1050.0	1033.4
air-conditioning & anti-icing	486.86	1.35804	15048.4	0.0	617.9
miscellaneous	237.43	0.66229	15048.4	0.0	617.9
crew & baggage	322.00	0.89819	3042.0	0.0	707.0
passenger cabin supplies	603.40	1.68312	5350.0	830.0	1030.0
safety equipment	238.00	0.66388	5350.0	830.0	1030.0
residual fuel port side	0.04	0.00010	13203.4	-4797.7	2340.0
residual fuel starboard side	0.04	0.00010	13203.4	4797.7	2340.0
passenger	80.00	0.22315	6972.8	1272.8	748.0
passenger		0.22315	7785.6	1272.8	748.0
passenger		0.22315	8598.4	1272.8	748.0
passenger		0.22315	9411.2	1272.8	748.0

PARTITION NAME	MASS [kg]	MASS/MTOW × 100%	Xcg [mm]	Ycg [mm]	Zcg [mm]
passenger	80.00	0.22315	10224.0	1272.8	748.0
passenger		0.22315	11036.8	1272.8	748.0
passenger		0.22315	11849.6	1272.8	748.0
passenger		0.22315	12662.4	1272.8	748.0
passenger		0.22315	13475.2	1272.8	748.0
passenger		0.22315	14288.0	1272.8	748.0
passenger		0.22315	15100.8	1272.8	748.0
passenger		0.22315	15913.6	1272.8	748.0
passenger		0.22315	16726.4	1272.8	748.0
passenger		0.22315	17539.2	1272.8	748.0
passenger		0.22315	6972.8	781.3	748.0
passenger		0.22315	7785.6	781.3	748.0
passenger		0.22315	8598.4	781.3	748.0
passenger		0.22315	9411.2	781.3	748.0
passenger		0.22315	10224.0	781.3	748.0
passenger		0.22315	11036.8	781.3	748.0
passenger		0.22315	11849.6	781.3	748.0
passenger		0.22315	12662.4	781.3	748.0
passenger		0.22315	13475.2	781.3	748.0
passenger		0.22315	14288.0	781.3	748.0
passenger		0.22315	15100.8	781.3	748.0
passenger		0.22315	15913.6	781.3	748.0
passenger		0.22315	16726.4	781.3	748.0
passenger		0.22315	17539.2	781.3	748.0
passenger		0.22315	6972.8	289.8	748.0
passenger		0.22315	7785.6	289.8	748.0
passenger		0.22315	8598.4	289.8	748.0
passenger		0.22315	9411.2	289.8	748.0
passenger		0.22315	10224.0	289.8	748.0
passenger		0.22315	11036.8	289.8	748.0
passenger		0.22315	11849.6	289.8	748.0
passenger		0.22315	12662.4	289.8	748.0

PARTITION NAME	MASS [kg]	MASS/MTOW × 100%	Xcg [mm]	Ycg [mm]	Zcg [mm]
passenger	80.00	0.22315	13475.2	289.8	748.0
passenger		0.22315	14288.0	289.8	748.0
passenger		0.22315	15100.8	289.8	748.0
passenger		0.22315	15913.6	289.8	748.0
passenger		0.22315	16726.4	289.8	748.0
passenger		0.22315	17539.2	289.8	748.0
passenger		0.22315	6972.8	-781.3	748.0
passenger		0.22315	7785.6	-781.3	748.0
passenger		0.22315	8598.4	-781.3	748.0
passenger		0.22315	9411.2	-781.3	748.0
passenger		0.22315	10224.0	-781.3	748.0
passenger		0.22315	11036.8	-781.3	748.0
passenger		0.22315	11849.6	-781.3	748.0
passenger		0.22315	12662.4	-781.3	748.0
passenger		0.22315	13475.2	-781.3	748.0
passenger		0.22315	14288.0	-781.3	748.0
passenger		0.22315	15100.8	-781.3	748.0
passenger		0.22315	15913.6	-781.3	748.0
passenger		0.22315	16726.4	-781.3	748.0
passenger		0.22315	17539.2	-781.3	748.0
passenger		0.22315	6972.8	-1272.8	748.0
passenger		0.22315	7785.6	-1272.8	748.0
passenger		0.22315	8598.4	-1272.8	748.0
passenger		0.22315	9411.2	-1272.8	748.0
passenger		0.22315	10224.0	-1272.8	748.0
passenger		0.22315	11036.8	-1272.8	748.0
passenger		0.22315	11849.6	-1272.8	748.0
passenger		0.22315	12662.4	-1272.8	748.0
passenger		0.22315	13475.2	-1272.8	748.0
passenger		0.22315	14288.0	-1272.8	748.0
passenger		0.22315	15100.8	-1272.8	748.0
passenger		0.22315	15913.6	-1272.8	748.0

PARTITION NAME	MASS [kg]	MASS/MTOW × 100%	Xcg [mm]	Ycg [mm]	Zcg [mm]
passenger	80.00	0.22315	16726.4	-1272.8	748.0
passenger	80.00	0.22315	17539.2	-1272.8	748.0
pass. bagage cargo hold 1	1394.67	3.89028	7785.4	0.0	-447.2
pass. bagage cargo hold 2	1405.33	3.92004	16761.2	0.0	-447.2
fuelload port inb. tank	1386.44	3.86733	12777.0	-1033.2	2340.0
fuelload starb. inb. tank	1386.44	3.86733	12777.0	1033.2	2340.0
fuelload port outb. tank	1167.05	3.25538	13440.4	-6889.6	2340.0
fuelload starb. outb. tank	1167.05	3.25538	13440.4	6889.6	2340.0
SUMMATION	35847.39	99.99271	12927.7	-20.8	1075.7
SUMMATION OEW + PAX	27940.40	77.93697	12963.7	-26.7	997.2
CG POSITION %MAC MTOW	26.02				
CG POSITION %MAC OEW + PAX	27.18				

Appendix 3: Three-view drawing of baseline design

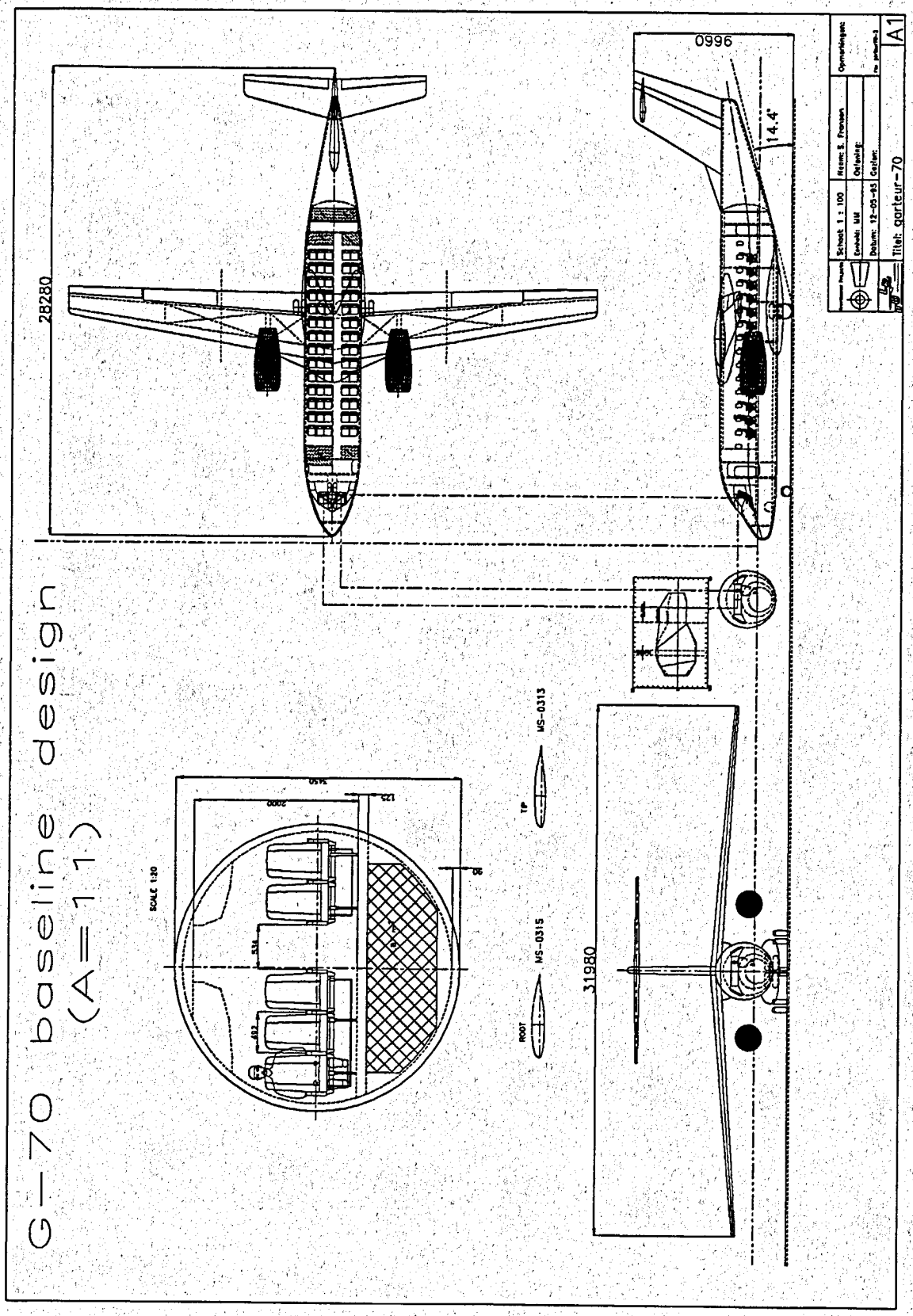

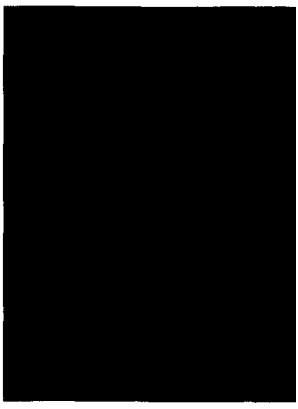

Memorandum 725
60142020935